

Effects of a dynamical role for exchanged quarks and nuclear gluons in nuclei: multinucleon correlations in deep-inelastic lepton scattering

Saul Barshay and Georg Kreyerhoff

III. Physikalisches Institut

RWTH Aachen

D-52056 Aachen

Germany

February 1, 2008

Abstract

It is shown that new data from the HERMES collaboration, as well as all of the earlier improved data from experiments concerning the EMC effect and shadowing in deep-inelastic scattering of leptons from nuclei, provide strong evidence for an explicit dynamical role played by exchanged quarks and nuclear gluons in the basic, tightly-bound systems of three and four nucleons, ^3He and ^4He . This opens the way for specific quark-gluon dynamics instigating multinucleon correlations in nuclei.

New experimental data have appeared [1], relating to the unusual behavior of nucleons and their constituents in atomic nuclei. The unusual behavior appears when nuclei are probed by deep-inelastic scattering of charged leptons[2, 3, 4, 5, 6]. The original discovery[2], called the “EMC effect”, is a depression below unity of the ratio of cross sections (per nucleon) $\frac{\sigma_A}{\sigma_D}$, for nucleus A as compared to deuterium, D. This occurs[2, 3] in the domain of momentum-fraction x , which is characteristic of valence quarks in a free nucleon, $x \gtrsim 0.25$. A depression in $\frac{\sigma_A}{\sigma_D}$ also occurs[4, 5] in the domain of small $x \lesssim 0.06$, at low and moderate Q^2 , the negative of the squared four-momentum transfer from the lepton. This effect is usually referred to as “shadowing”. An effect of this kind is expected at small x , at and near to $Q^2 = 0$, as a geometrical effect of the nuclear surface, which diminishes the intensity of vector-meson-like components of the photon through strong interactions with nucleons near to this surface^{F1}. From the very beginning[2, 3] of the experimental measurements, there have been two important observations (which often have not been emphasized in subsequent work):

- (1) The “EMC effect” is conspicuously prominent[3, 4] in the basic nucleus ^4He ; its growth with A in going to ^{40}Ca and to ^{119}Sn is moderate. A corollary to this is the matter of possible dependence upon Q^2 of the loss of momentum fraction from valence quarks in nuclei. There have been indications in the data[7], that a small additional loss occurs as Q^2 is increased, that is $\frac{\sigma_A}{\sigma_D}$ is depressed further below unity. This effect, although small, is “important because of its direction: if the loss of valence-quark momentum fraction increases with Q^2 , the underlying dynamics can hardly be solely conventional nuclear physics”. [7]

^{F1}This particular effect, accomodated by conventional concepts in nuclear physics, is not dealt with in this paper, except for an observation at the end concerning a possible difference between “shadowing” for real photons ($Q^2 = 0, \vec{Q} \neq 0$) and for virtual photons with Q^2 near zero ($\vec{Q} \rightarrow 0$).

- (2) There have been indications in data[8, 9] of a rather sharp and strong drop of $\frac{\sigma_A}{\sigma_D}$ below unity, in the domain $0.01 < x < 0.1$ for $0.05 < Q^2 < 1.5(\frac{\text{GeV}}{c})^2$. This suggests the possibility that an important part of the “shadowing” effect has an origin in specifically partonic dynamics within nuclei, an origin that should be a natural extension of the partonic dynamics which leads to the loss of momentum fraction in the x -domain of the valence quarks[7].

The above facts point to the possibility that quark-gluon degrees of freedom contribute explicitly to multinucleon correlations[10] and forces[11] in nuclei. These correlations[10] and forces are prominently present already in the basic, tightly-bound He nuclei. When one recalls that the maximum nucleon densities encountered in ^3He and ^4He are about two times higher than those in any other nucleus, it is not surprising that if relatively short-range, three-body correlations of quark-gluonic origin exist, there are significant effects observable in these systems, in particular when probed by deep-inelastic lepton scattering. This was the basis for a detailed phenomenological model[10] for a three-nucleon correlation (force[11]) which involved as dynamics the exchange of one quark from each nucleon, under the influence of nuclear gluon interactions ^{F2}. Momentum fraction is lost from charged constituents to the quanta of a nuclear gluonic field.

The dynamical model offers the possibility of understanding the essential EMC effect at $x > 0.25$, and also a part of the shadowing-like effect, in a unified picture[7]. A quantitative description (on a χ^2 basis) of all of the nuclear data in the domain $0.02 \leq x \leq 0.7$ was achieved with a few parameters whose values are estimated *a priori* from physical considerations, and whose fit values agree with these estimates[10]. The A-dependence of $\frac{\sigma_A}{\sigma_D}$ is successfully predicted, as has been shown by the detailed analyses of data by Smirnov[12]. New predictions are made[10]. One, which has been experimentally verified[13, 7], involves the close similarity between $\frac{\sigma_A}{\sigma_D}$ for the “irregular” nucleus ^6Li and that for ^4He . The nucleus ^6Li is irregular in having an r. m. s. radius of ~ 2.5 fm, about the same as that for ^{12}C . Thus, if viewed as a system of uniform nucleon density, this density is low, about one-half that of ^4He . From this point of view, one would expect little reduction in $\frac{\sigma_A}{\sigma_D}$ for ^6Li . Instead the data show that on “a bin to bin comparison the $\frac{^6\text{Li}}{^4\text{He}}$ ratio is consistent with unity over the common x range”[13] ($0.01 \lesssim x \lesssim 0.5$). (Note Fig. 1 of Ref. 7.) Thus, as probed by deep-inelastic lepton scattering, ^6Li behaves as if composed of a ^4He -like group (and/or ^3He -like groups) of nucleons.

Quantitative examples of the increased loss of momentum fraction from valence quarks (reaching a limit) with increasing Q^2 , were given in Figs. 7, 8 of Ref. 10, for ^4He and ^{12}C in particular. The new data from HERMES[1] give the most distinct indication of this effect, for ^3He and ^{14}N , over the range $1 < Q^2 < 20(\frac{\text{GeV}}{c})^2$, for $\langle x \rangle \sim 0.4$. We describe this below. The new data from HERMES[1] exhibit a sharp and strong drop of $\frac{\sigma_A}{\sigma_D}$ below unity for $x < 0.06$. The data show a marked Q^2 dependence of this effect for (average) x values in the domain $0.01 < \langle x \rangle < 0.06$. What is strikingly unusual is that the depression of $\frac{\sigma_A}{\sigma_D}$ in this domain of $\langle x \rangle$, first increases as Q^2 moves up from near zero, $0.3 < Q^2 < 1.5(\frac{\text{GeV}}{c})^2$. A principal purpose of this paper is to describe this effect quantitatively, and to discuss physically two possible, complementary origins of such unusual Q^2 dependence. This is done below, within the unified framework provided by the model for three-nucleon correlations which originate in explicit quark-gluon dynamics, in ^3He in particular. The new HERMES data[1] show that $\frac{\sigma_A}{\sigma_D}$ already falls significantly below unity in ^3He , as in ^4He , which was anticipated[10, 12].

To start the analysis, we briefly explain the essential physical features of the

^{F2}A diagrammatic representation is in Fig. 2 of Ref. 7 and Fig. 2 of Ref. 10

formula^{F3} for $\frac{\sigma_A}{\sigma_D}$ which provides a quantitative description of all of the nuclear data in the domain $0.02 \leq x \leq 0.7$, for $1 < Q^2 < 100(\frac{\text{GeV}}{c})^2$.

$$\begin{aligned} \frac{\sigma_A(x, Q^2)}{\sigma_D(x, Q^2)} = 1 & - \delta(A) \left\{ \frac{3.3\sqrt{x}(1-x)^3 - C(Q^2)f(Q^2, x^2)\sqrt{x}e^{-Bx^2}}{3.3\sqrt{x}(1-x)^3 + 1.1(1-x)^7} \right\} \\ & - \delta(A) \left\{ \frac{1.1(1-x)^7 - \tilde{C}x^\beta e^{-B'x^2}}{3.3\sqrt{x}(1-x)^3 + 1.1(1-x)^7} \right\} \end{aligned} \quad (1)$$

with $B = 11.3$, $B' = 35$, $\beta = 0.35$,

$$\delta(A) = 0.27 \left\{ 1 - \frac{1}{A^{1/3}} - \frac{1.145}{A^{2/3}} + \frac{0.93}{A} + \frac{0.88}{A^{4/3}} - \frac{0.59}{A^{5/3}} \right\}$$

and

$$\begin{aligned} C(Q^2) &= \frac{3}{\int_0^1 \frac{dx}{x} \sqrt{x} e^{-11.3x^2} f(Q^2, x^2)} \\ f(Q^2, x^2) &= e^{-48x^4 \left(\frac{\ln(Q^2/2)}{\ln(Q^2/0.04)} \right)} \\ \tilde{C} &\cong \frac{1.1 \int_{0.06}^1 \frac{dx}{x} (1-x)^7}{\int_{0.06}^1 \frac{dx}{x} x^{0.35} e^{-35x^2}} \end{aligned}$$

In this formula for $\frac{\sigma_A}{\sigma_D}$, the second term modifies the usual valence-quark distribution [14] of momentum fraction. While maintaining the valence-quark number through $C(Q^2)$, a fraction $\delta(A)$ of the valence quarks (per nucleon) are removed from the usual distribution for a free nucleon, and are distributed instead in a Gaussian form^{F4} characterized by a size parameter B ; the size characterizes the spatial motion of a fraction of the quarks in a correlated, three-nucleon system. The fit parameter corresponds to a spatial dimension ($\cong \sqrt{3B}/m_N$) of about 1.2 fm, the same as that estimated *a priori* from geometrical considerations concerning a three-nucleon correlation[10], (and is well within the r. m. s. charge radius of ^3He , which is about 1.7 fm). The modification results in a gradual depression of $\frac{\sigma_A}{\sigma_D}$ below unity in the valence-quark domain, $x \gtrsim 0.3$. This depression increases a little with increasing Q^2 , in particular in the domain $1 < Q^2 < 20(\frac{\text{GeV}}{c})^2$, reaching a limiting depression from above, as is illustrated in Figs. 7, 8 of Ref. 10 for ^4He and ^{12}C , respectively. The effect, which is due to $f(Q^2, x^2)$ in the second term in Eq. (1), arises physically because the correlation among valence quarks and nuclear gluons, as seen by a high- Q^2 probe, can be considered to be an additional nuclear degree of freedom, whose x -distribution “softens” as Q^2 increases due to more momentum fraction being lost to nuclear gluons. In $f(Q^2, x^2)$, the loss is limited by the decreasing

^{F3}In the comparison with data carried out in Ref. 10, this formula is identified with the ratio of structure functions $\frac{F_2^A(x, Q^2)}{F_2^D(x, Q^2)}$. This is identical with $\frac{\sigma_A}{\sigma_D}$ if the ratio of longitudinal to transverse

deep-inelastic scattering cross sections $\tilde{R}^A = \frac{\sigma_L^A}{\sigma_T^A}$ satisfies $\tilde{R}^A(x, Q^2) = \tilde{R}^D(x, Q^2)$ (or independently of such an equality, if $Q^2 \rightarrow 0$). Here, we use the phenomenological formula for $\frac{\sigma_A}{\sigma_D}$, and we explicitly discuss the matter (Ref. 1) of $\tilde{R}^A(x, Q^2)$ possibly not equal to $\tilde{R}^D(x, Q^2)$ later in this paper.

^{F4}The approximation of using a Gaussian form in momentum space is based upon an approximate Gaussian form for quark motion in configuration space in the three-nucleon correlation. The Gaussian form is not zero at $x = 1$, but the contribution of this term to σ_A is then $\propto e^{-11.3}$, which is negligible compared to the non-zero contribution at $x = 1$ due to the nuclear Fermi motion. The Gaussian form does simulate the effect of Fermi motion in the ratio $\frac{\sigma_A}{\sigma_D}$, causing it to move sharply upward above unity as $x \rightarrow 1$.

strength of the gluon coupling, $\alpha_s(Q^2) \propto \frac{1}{\ln(Q^2/0.04)}$ (for $\Lambda_{\text{QCD}} \sim 200 \frac{\text{MeV}}{c}$)^{F5}. The A dependence is given by the function $\delta(A)$, which uniquely arises by excluding from the three-nucleon correlation the number of nucleons A_S , which reside in the (relatively diffuse) surface of a large nucleus, that is[10] $\delta(A) = N(1 - \frac{A_S}{A})$. The single, overall normalization parameter, $N = (27 \pm 6)\%$, is fit[10] to $\delta(A = 4) = 6^{+1.5}_{-1}\%$. (Then, $\delta(A = 14) \cong 12.6\%$ and $\delta(A = 3) \cong 4.2\%$.) Let us look now at the HERMES data[1], shown in Figs. 1,2 for ^{14}N and ^3He , respectively. For $\langle x \rangle \sim 0.4$, well into the domain of valence-quark momentum fraction, the data indicate that $\frac{\sigma_A}{\sigma_D}$ falls up to 4% more below unity as Q^2 goes up from ~ 1 to $\sim 20(\frac{\text{GeV}}{c})^2$. For ^3He , the additional drop may be up to 2%.^{F6} These numbers appear similar to those calculated from Eq. (1) ten years ago[10], in the Figs. 8, 7 for ^{12}C and ^4He , respectively.

The physical picture of a three-nucleon correlation of quark-gluonic origin allows for the natural prediction of a shadowing-like effect, in fact a rather sharp drop of $\frac{\sigma_A}{\sigma_D}$ below unity, for $x < 0.06$. [10] This is contained in the last term in Eq. (1). A colored agglomeration of sea quarks (antiquarks) is exchanged from each nucleon, instead of a valence quark, under the influence of nuclear gluon interactions. The fraction of the sea (taken as $\delta(A)$ in Eq. (1)) involved in this dynamics is removed from the relevant momentum-fraction distribution [14] for a free nucleon and is distributed instead in a form given by the x -dependence multiplying \tilde{C} in Eq. (1). The crucial point is the non-zero power of x , $\beta > 0$. Physically, this means that whereas the number of sea quarks and antiquarks in an individual nucleon is formally infinite (i. e. $\propto \int_0^1 \frac{dx}{x} \dots$), the number of these which are involved in the three-nucleon correlation is finite. In the representation for $\frac{\sigma_A}{\sigma_D}$ in Eq. (1), it is the factor x^β which results in the relatively sharp drop below unity for $x < 0.06$.^{F7} The factor $\tilde{C}(Q^2)$ ensures that the number of sea quarks and antiquarks involved in the larger spatial domain of the three-nucleon correlation is equal to the number removed from the individual nucleon distribution. The “size” parameter B' in the Gaussian, characterizing the spatial motion of the sea, is expected to be larger than B ; the fit number corresponds to a dimension of about 2.2 fm (B' may increase[10] somewhat with A .) Eq. (1) resulted[10] in a representation with $\chi^2 \lesssim 1$ per degree of freedom, for all of the nuclear data taken with Q^2 between about 2 and 100 $(\frac{\text{GeV}}{c})^2$, for x in the domain $0.02 \leq x \leq 0.7$.^{F8}

Now the HERMES data[1] exhibit a new Q^2 dependence for $0.3 < Q^2 < 1.5(\frac{\text{GeV}}{c})^2$, with x in the domain $0.0126 \leq x \leq 0.055$, as shown by the first 6 graphs in Figs. 1,2 for ^{14}N and ^3He , respectively. When averaged over the relevant Q^2 , the fall of $\frac{\sigma_A}{\sigma_D}$ below unity is even sharper and deeper[1] than in most of the earlier data[4, 5]. We show here that the unusual behavior as a function of Q^2 , at small x , can be well represented by a simple, overall form factor, and a normalization change, multiplying the last term in Eq. (1). The modification is

$$\delta(A) \times 1 \rightarrow 6.3\delta(A)F(Q^2) \quad (2)$$

^{F5} $f(Q^2, x^2) = 1$ for $Q^2 = 2(\frac{\text{GeV}}{c})^2$, and is taken as 1 for Q^2 below this value in the present analysis of the new data down to $Q^2 \sim 0.3(\frac{\text{GeV}}{c})^2$.

^{F6} These are small changes which might be ignored[1], within the experimental uncertainties. Nevertheless, the direction is in accord with earlier experimental indications[7], and the changes are expected within a model of explicit quark-gluon correlations in nuclei. Note also the Q^2 dependence of the ^{119}Sn data for $0.4 < x < 0.5$, in Fig. 4 of M. Arneodo et. al. (NMC), Nucl. Phys. **B481**, 23 (1996).

^{F7} The fit parameter β is restricted by $0 < \beta < \frac{1}{2}$, because the distribution of momentum fraction in the sea is “softer” than that for the valence quarks ($\propto \sqrt{x}$), as $x \rightarrow 0$. The initial sea is taken for $x \geq 0.06$.

^{F8} At smaller x , one encounters the need to deal explicitly with the geometrical shadowing effect which is present already for real photons ($Q^2 = 0$, $\vec{Q} \neq 0$).^{F1}

with

$$F(Q^2) = \frac{4Q^2}{Q^2 + 1} \frac{1}{Q^2 + 1} = 4 \left\{ 1 - \frac{1}{Q^2 + 1} \right\} \frac{1}{Q^2 + 1}, \quad Q^2 \text{ in } \left(\frac{\text{GeV}}{c} \right)^2$$

Keeping all parameters[10] fixed, the curves which result from Eqs. (1,2) are superimposed on data in Figs. 1,2. Significant aspects of the data both in the valence-quark x domain and in the shadowing domain are evident in the curves. At the lowest values of $\langle x \rangle$, the curves are meant to refer specifically to the new HERMES data[1]. The NMC[4] and E665[5] data involve a much higher lepton-beam energy, whereas possible explicit dependence upon this energy is suppressed in the phenomenological Eqs. (1,2). The data at these higher energies and at low Q^2 , may be expected to be closer to unity because the kinematic variable $\epsilon(x, Q^2, E)$ which appears in the ratio of cross sections (as discussed in the next paragraph), is close to unity, thus removing sensitivity^{F3} to $\tilde{R}^A(x, Q^2)$. A possible physical reason for the presence of a form factor which vanishes not only as $Q^2 \rightarrow \infty$, but also[11] as $Q^2 \rightarrow 0$ (this is the unusual aspect in Eq. (2)), lies in a high degree of coherence associated with the system of exchanged sea partons, and nuclear gluons (which are individually, colored quanta). This occurs when the system at small values of x responds to a low- Q^2 probe. Qualitatively, exchange of colored quanta (or aggregates) initially at small x , involve spatial dimensions of the order of $\frac{1}{m_N x} = \text{many fermis}$. Thus coherence over a nucleus, and consequently a form factor falling at least like approximately $1/Q^2$, may be expected. However, in addition there is the confinement axiom. Starting with a system of nucleons, individual colored entities cannot be present over extended dimensions within this system. This suggests that a probe with $Q^2 = 0$ ($\vec{Q} = 0$) “sees” no color-induced correlation. Then, the remaining shadowing is related to colorless aggregates of quarks which constitute the low-mass vector meson components of the photon. Such behavior is incorporated phenomenologically in a simple way in Eq. (2); with $F(Q^2)$ normalized to unity at its maximum, which occurs at $Q^2 = 1(\frac{\text{GeV}}{c})^2$ for this form. Note that averaging $6.3\delta(A)F(Q^2)$ over Q^2 in the interval $0.3 < Q^2 < 1.5(\frac{\text{GeV}}{c})^2$, gives an effective, A-dependent coefficient of the last term in Eq. (1) of $\sim 6.1\delta(A)$ (instead of $\delta(A)$); this accounts quantitatively for the increased depth of the sharp drop for $x < 0.06$ in the HERMES data[1] (their Fig. 1) as compared to the earlier data[4, 5]^{F9}. At $x \cong 0.01$ the earlier depression of $\frac{\sigma_A}{\sigma_D}$ below unity by about 6% for ^{12}C is increased to about 35% for ^{14}N in the HERMES data[1]!

Within the physical picture embodied in Eq. (1), we consider the interpretation of the new data in terms^{F3} of $\tilde{R}^A(x, Q^2) > \tilde{R}^D(x, Q^2)$, as given in the analysis[1] by the HERMES collaboration. The ratio $\frac{\sigma_A}{\sigma_D}$ is written in terms of the ratio of structure functions F_2 , times a multiplicative factor

$$\frac{\sigma_A(x, Q^2)}{\sigma_D(x, Q^2)} = \frac{F_2^A(x, Q^2)}{F_2^D(x, Q^2)} \left\{ \frac{(1 + \epsilon \tilde{R}^A(x, Q^2))(1 + \tilde{R}^D(x, Q^2))}{(1 + \epsilon \tilde{R}^D(x, Q^2))(1 + \tilde{R}^A(x, Q^2))} \right\} \quad (3)$$

where $\epsilon(x, Q^2, E)$ is the kinematic variable related to the virtual-photon polarization, defined by HERMES in their Eq. (2), [1] with $0 \leq \epsilon \leq 1$; (E is the initial-lepton laboratory energy). The factor multiplying $\frac{F_2^A}{F_2^D}$ is unity independently of the value

^{F9} Averaging $6.3\delta(A)F(Q^2)$ over Q^2 in the interval $1 < Q^2 < 100(\frac{\text{GeV}}{c})^2$ gives an effective, A-dependent coefficient of the last term in Eq. (1) of $\sim \delta(A)$, in agreement with the representation of the earlier data[10]. It is worth noting that the fit normalization parameter $N \sim 0.3$ in the factor $\delta(A)$ which multiplies the valence-quark term in Eq. (1), contains a factor of $\frac{1}{3}$ corresponding to the *a priori* probability for involving a single valence quark from each nucleon in the correlation (at any instant). This constraint does not hold for the sea quark normalization as changed in Eq. (3); the fit normalization here is of order unity.

of $(\tilde{R}^A - \tilde{R}^D)$, when the kinematic variable ϵ becomes unity; this is formally at $Q^2 = 0$. As ϵ moves towards zero, which occurs for larger Q^2 in the HERMES data, the factor becomes less than unity if $\tilde{R}^A(x, Q^2) > \tilde{R}^D(x, Q^2)$. However, if $(\tilde{R}^A - \tilde{R}^D)$ becomes effectively zero already at moderate values of Q^2 , then the multiplicative factor is again unity, independently of the value of ϵ .^{F10} Assuming that an interpretation of the new data in terms of $(\tilde{R}^A - \tilde{R}^D) > 0$ is valid, we make an approximate identification of Eq. (3) with the successful phenomenological formula in Eq. (1), modified as in Eq. (2). Then, for \tilde{R}^D and \tilde{R}^A less than unity, we obtain an approximate relation in the domain $x < 0.06$, with $Q^2 < 1.5(\frac{\text{GeV}}{c})^2$, for a function^{F11} $\Delta(x, Q^2)$, at given E

$$\Delta(x, Q^2) = \{1 - \epsilon\} (\tilde{R}^A - \tilde{R}^D) \sim 6.3\delta(A)s(x) \left\{1 - \frac{1}{Q^2 + 1}\right\} \left(\frac{1}{Q^2 + 1}\right) \quad (4)$$

where

$$s(x) = \frac{1.1(1-x)^7 - \tilde{C}x^{0.35}e^{-35x^2}}{3.3\sqrt{x}(1-x)^3 + 1.1(1-x)^7}$$

The quantity on the right in $\{\dots\}$ has correct limiting behaviors to phenomenologically, approximately represent $\{1 - \epsilon\}$ i. e. $\epsilon = 1$ at $Q^2 = 0$, and $\epsilon \rightarrow 0$ for large Q^2 (at given E and $\langle x \rangle$). The explicit dependence upon E and $\langle x \rangle$ is suppressed in this approximation; the numerical values of ϵ are roughly given as in the HERMES data for the lowest $\langle x \rangle$ -bins[1]. At fixed small x , Eq. (4) suggests for the ratio

$$\left\{ \frac{\tilde{R}^A(x, Q^2)}{\tilde{R}^D(x, Q^2)} - 1 \right\} \propto \delta(A) \left(\frac{1}{Q^2 + 1} \right) \quad (5)$$

Eq. (5) is an approximate representation^{F11} of the growth at low Q^2 for the ratio at small x , which is extracted from the Q^2 variation of $\frac{\sigma_A}{\sigma_D}$ by HERMES using some assumptions^{F10} (in the upper part of their Fig. 5).[1] It is possible that $\frac{\tilde{R}^A}{\tilde{R}^D}$ falls again as Q^2 approaches zero. Furthermore it is notable that the extracted increase[1] in the ratio in going from He to ^{14}N is approximately given by $\frac{\delta(A=14)}{\delta(A=4)} \cong 2$, in accord with Eq. (5). The interpretation of the data in terms of $\tilde{R}^A > \tilde{R}^D$ is strengthened by the likelihood of an enhancement in the interaction of longitudinal photons with the correlated sea among three nucleons, for the reasons given below. With respect to the Q^2 domain of the HERMES data at small $\langle x \rangle$, one might assume that the multiplicative factor in Eq. (3) is unity, and attribute the behavior of their basic data for $\frac{\sigma_A(x, Q^2)}{\sigma_D(x, Q^2)}$ shown here in Figs. 1,2, to an unusual, strong variation with low Q^2 , at small x , of $\frac{F_2^A(x, Q^2)}{F_2^D(x, Q^2)}$, as in a form factor with the general limiting behavior of $F(Q^2)$ in Eq. (2). However, then the Q^2 dependence of the data taken at higher beam energies[4, 5] is not represented at small $\langle x \rangle$ and moderate Q^2 (by our simple $F(Q^2)$).

In fact, assuming the validity of the interpretation in terms of $\tilde{R}^A > \tilde{R}^D$, also allows for a definite argument that there is new physics involving multinucleon correlations from explicit quark-gluon dynamics in nuclei. Interaction of the virtual photon with a single “isolated” quark, largely involves no helicity-flip; then angular

^{F10}This is in fact, the situation for the values of $\frac{\tilde{R}^A(x, Q^2)}{\tilde{R}^D(x, Q^2)}$ extracted by HERMES under certain assumptions concerning the behavior of $\frac{F_2^A(x, Q^2)}{F_2^D(x, Q^2)}$ and $\frac{\tilde{R}^A(x, Q^2)}{\tilde{R}^D(x, Q^2)}$. [1] Thus, a strong variation at low Q^2 which is evident in the HERMES data in Figs. 1,2, then occurs in $\frac{\tilde{R}^A}{\tilde{R}^D}$.

^{F11}The more complete form of the right-hand side of Eq. (4) resulting from Eqs. (1,2) has two zeros: one at $Q^2 \cong 0.043(\frac{\text{GeV}}{c})^2$ which corresponds to $\epsilon \rightarrow 1$; the other at $Q^2 \cong 23(\frac{\text{GeV}}{c})^2$ which corresponds to $\tilde{R}^A(x, Q^2) \rightarrow \tilde{R}^D(x, Q^2)$.

momentum conservation requires that the interaction be with a transverse photon (as is most easily seen in the “brick wall” system for the photon-quark collision). This constraint does not hold in a multiquark correlation, where the struck quark is not “free”, but rather propagates, emits a gluon, and propagates to another nucleon. An exercise involving only Clebsch-Gordon coefficients indicates that if the spin-orientation of an interacting system of three quarks (nucleons) does not change, then interaction with a longitudinal photon (behaving like a spin-zero quanta) is favored over a transverse photon by an *a priori* factor of $\frac{3}{2}$. There can also be a dynamical enhancement of longitudinal photons in interaction with aggregates of sea. By comparing initial-interaction coefficients of longitudinal and transverse virtual-photon polarization, we estimate an enhancement factor of the order of

$$\left\{ \frac{((m_N x)^2 + \tilde{m}_q^2)^{1/2}}{(m_N x)} \tilde{f}(Q^2) \right\}^2 \sim 2,$$

in the small- $\langle x \rangle$, low- Q^2 domain of HERMES, for an effective aggregate mass \tilde{m}_q of ~ 20 MeV (\tilde{f} is a form factor), with m_N the nucleon mass (therefore $m_N x \sim 20$ MeV for $x \sim 0.02$).

A final remark concerns the shadowing at $Q^2 = 0$ for real photons, when compared to that for virtual photons with Q^2 near to zero. If the explicit partonic effect first gives increasing shadowing as Q^2 moves away from zero, then this effect on top of the conventional geometric effect already present for real photons, would give somewhat more shadowing for the virtual photons. There may be some experimental evidence for this[8, 15]. In addition, since the geometric shadowing effect at a given very small x is expected to become less with a marked increase in Q^2 , if the partonic shadowing effect initially increases away from $Q^2 = 0$, then the overall shadowing effect will show a reduced variation with increasing Q^2 .

In summary, when viewed and quantitatively correlated within a unified physical picture, the new data, and all of the earlier improved data from experiments over the last ten years concerning the EMC effect and shadowing, provide the best evidence yet for an explicit dynamical role played by exchanged quarks and nuclear gluons in atomic nuclei.

We thank the HERMES collaboration for information, in particular Prof. M. Düren and Dr. G. van der Steenhoven.

References

- [1] HERMES Collab, K. Akerstaff et al., hep-ex/9910071, Nov. 1999
- [2] J. J. Aubert et al. (EMC), Phys. Lett. **B123** (1983), 275
- [3] A. Bodek et al., Phys. Rev. Lett. **50** (1983), 1431; **51** (1983), 534
R. G. Arnold et al. , Phys. Rev. Lett. **52** (1984), 727
- [4] P. Amaudruz et al. (NMC), Nucl. Phys. **B441** (1995) , 3
- [5] M. R. Adams et al. (E665), Z. Phys. **C67** (1995), 403
- [6] J. Gomez et al. (SLAC), Phys. Rev. **D49** (1994), 4348
- [7] This is emphasized, with a summary of the relevant data, in S. Barshay and D. Rein, Particle World **4** (1994), 3
- [8] J. Franz et al., Z. Phys. **C10** (1981), 105
J. Bailey et al., Nucl. Phys. **B151** (1979), 367

- J. Eickmeyer et al., Phys. Rev. Lett. **36** (1976), 289
 S. Stein et al., Phys. Rev. **D12** (1975), 1884
- [9] M. S. Goodman et al., Phys. Rev. Lett. **47** (1981), 293
- [10] S. Barshay and D. Rein, Z. Phys. **C46** (1990), 215
- [11] S. Barshay, Phys. Lett. **100B** (1981), 276
- [12] G. Smirnov, Phys. Lett. **B364** (1995), 87
 G. Smirnov, Yad. Fiz. **58**, no. 9 (1995), 1712; Phys. At. Nucl. (Engl. translation) **58**, no. 9 (1995)
 See also hep-ph/9611203. This author has also argued from the data for a basic dynamical role in the He nuclei.
- [13] P. Amaudruz, et al. (NA37/NMC), Z. Phys. **C53** (1992), 73
- [14] CDHS Collab. , J. G. H. de Groot et al., Z. Phys. **1** (1979), 143
 H. Abramowitz et al., Z. Phys. **C17** (1983), 283
- [15] L. Criegee et al., Nucl. Phys. **B121** (1977), 38

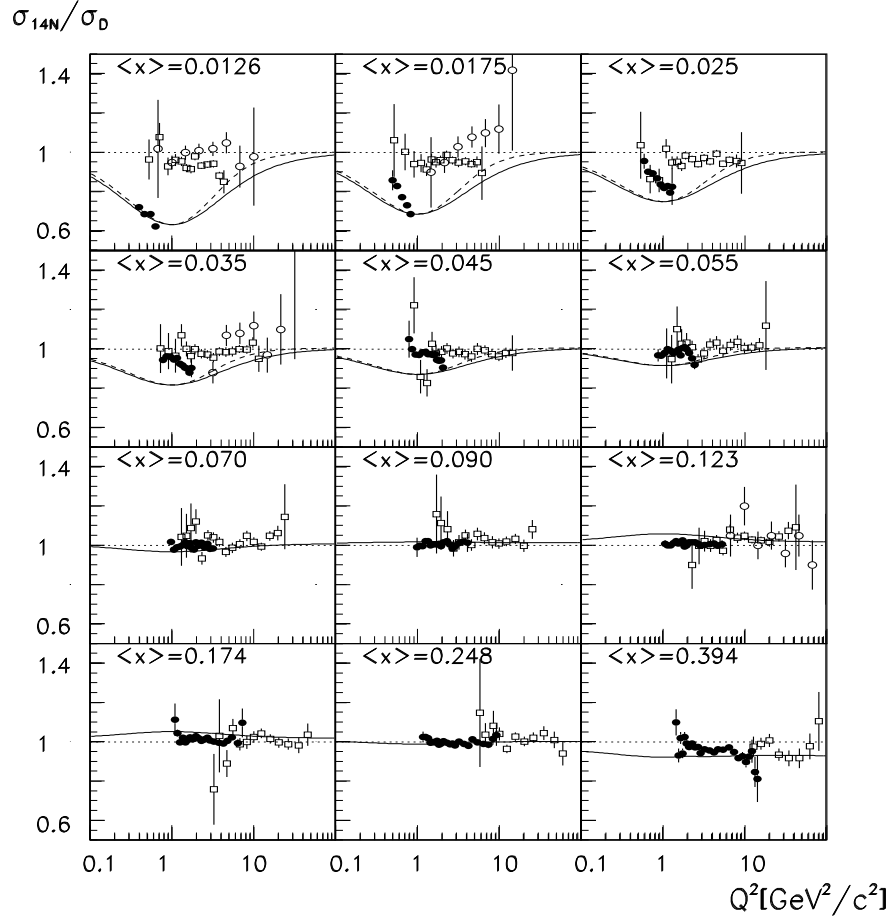


Figure 1: The ratio of cross section for inclusive deep-inelastic lepton scattering from ^{14}N to that of ^2H , versus Q^2 for specific x -bins: the solid circles are HERMES data[1]. The open squares are NMC data[4] for ^{12}C and the open circles are E665 data[5] for ^{12}C . The solid curves are calculated from Eqs. (2,3) for $A = 14$. The dashed curves illustrate a form factor with a stronger fall-off at large Q^2 : $F(Q^2) = \frac{27Q^2}{(Q^2+2)^3}$.

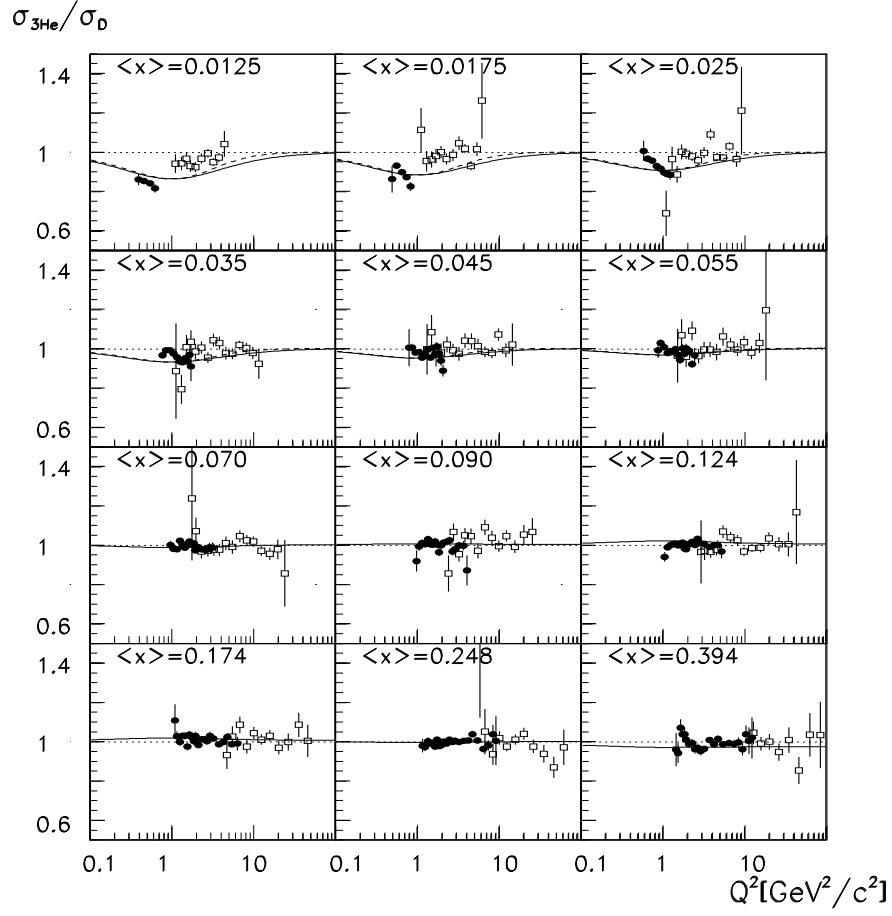


Figure 2: The ratio of cross section for inclusive deep-inelastic lepton scattering from ${}^3\text{He}$ to that for ${}^2\text{H}$, versus Q^2 for specific x -bins: the solid circles are preliminary HERMES data (<http://dxhra1.desy.de/notes/pub/trans-public-subject.html>). The open squares are NMC data[4] for ${}^4\text{He}$. The solid curves are calculated from Eqs. (2,3) for $A = 3$. The dashed curves illustrate a form factor with a stronger fall-off at large Q^2 : $F(Q^2) = \frac{27Q^2}{(Q^2+2)^3}$.